

Electromechanical Coupling Dynamic Model and Speed Response Characteristics of the Flexible Robotic Manipulator

Yufei Liu^{1,2(✉)}, Bin Zi², Xi Zhang³, and Dezhang Xu¹

¹ School of Mechanical and Automotive Engineering,
Anhui Polytechnic University, Wuhu 241000, China
Liuyufeia@ahpu@126.com

² School of Mechanical Engineering,
Hefei University of Technology, Hefei 230009, China

³ Engineering Research and Training Center, Anhui Polytechnic University,
Wuhu 241000, China

Abstract. The flexible robotic manipulator, which has the advantages of lightweight, flexible operation and low energy consumption, is a typical electromechanical coupling system containing the driving system, transmission system and flexible manipulator. Considering the driving motor, transmission system and flexible manipulator as an integrated object, the electromechanical coupling dynamic model of the flexible robotic manipulator system (FRMS) was constructed based on the overall coupling relationship and electromechanical dynamics analysis approach. To reveal the electromechanical coupling mechanism of the FRMS, the speed response characteristics under electromechanical coupling effects are presented. The results indicate that the electromechanical coupling factors have significant impacts on the dynamic property of the FRMS, which are meaningful for the design and control of flexible robotic manipulators.

Keywords: Robotic · Flexible manipulator · Electromechanical coupling dynamic

1 Introductions

The robotic manipulators have widely application, such as mechanical processing, precision assembly, loading and spraying [1, 2]. Because the operation task is completed through the manipulator and its actuators, the structure and dynamic characteristics of the robotic manipulator have important effect on the performance of the whole system. As the modern robot technology developing to lower energy consumption, higher speed and higher precision, the robotic manipulator should be able to sustain the operation accuracy over a long period of time in the process of performing operations [3–5]. In order to realize the position precision of the actuators, traditional robotic manipulators are usually designed with rigid structure. However, the structural vibration during operations, start-stop and motion transformation, especially in high-speed operation, seriously reduces the operation accuracy and precision of the

robotic manipulator [2]. Meanwhile, owing to the poor vibration controllability of the rigid manipulator, the structural vibration may persist for a long time which obviously limits the efficiency of the system. Besides, because the materials of the rigid manipulator are heavy, it will consume relatively more energy in high speed motion and wide range of space operation tasks [1, 6].

With the rapid development of modern manufacturing equipment, there has increasing attention been focused on the flexible manipulator which is a typical flexible structure [7]. The flexible manipulator can significantly reduce the weight of the structure while assure multi-function and has been widely used in the large lightweight structure, extending from the field of aeronautics and astronautics to the micro-operation robot and precision manufacturing with the development of modern industry and engineering applications [1, 8]. Due to the use of lightweight materials, however, the flexible manipulator usually has low stiffness and damping and exhibits residual vibrations during the operation. Therefore, the dynamic characteristics and control strategies for the flexible manipulator are the key problems for realizing the full advantages of its lightweight.

The flexible robotic manipulator is a typical complex electromechanical system which has complex electromechanical coupling relationship between the servo drives and the actuators [9]. For example, in the permanent magnet AC servo system, there is obvious coupling relationship between the mechanical parameters of the structure and the electromagnetic parameters of the driving system, whose concrete form can be divided into the coupling between the harmonic current in the armature circuit of the driving system and the transmission system, the coupling between the control parameters of the motor speed regulation system and the mechanics parameters of the servo system as well as the coupling between the servo system and the load system. These electromechanical coupling relationships of the flexible robotic manipulator system (FRMS) are easy to arouse the system vibration and affect the system dynamic characteristics [10]. Moreover, the systematic excitation caused by the coupling factors will be more prominent for high-speed and light structures, due to its low mode property and flexible factors, flexible robotic manipulator is easy to cause low resonance phenomenon which has obvious influence on the dynamic characteristics. However, most of the existing investigations considering the dynamic modeling and vibration control of the flexible robotic manipulator usually ignore the effect of the dynamic characteristics of driving system [11–13]. In order to accurately reflect the real dynamic characteristics of the FRMS, the electromechanical coupling factors should be considered. This paper considers the driving motor, transmission system and flexible manipulator as an integrated object, and based on the overall coupling relationship and electromechanical dynamics analysis approach, the electromechanical coupling dynamic model was constructed. To reflect the electromechanical coupling mechanism of the FRMS, the speed response characteristics of the FRMS under electromechanical coupling effects are revealed.

2 Electromechanical Coupling Dynamic Equation of the FRMS

Figure 1 shows the electromechanical coupling diagram of a permanent magnet synchronous motor (PMSM) - driven FRMS.

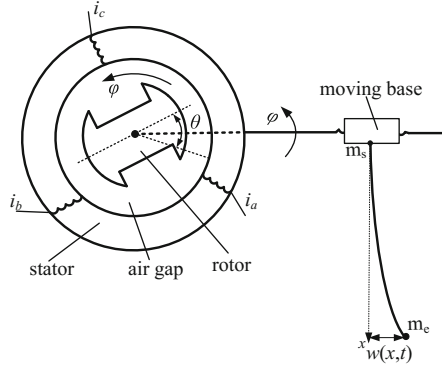


Fig. 1. Structure physical model of the FRMS

The AC servomotor is mainly composed of stator and rotor. When flowed through three-phase sinusoidal alternating current of 120 phase difference, the stator flux produces space rotating magnetic field whose rotating speed is associated with the frequency of the current. Then, through the driving torque produced by the interaction between stator magnetic field and rotor magnetic field, the electric energy is changed into the mechanical energy and can be used to drive the flexible manipulator.

The electromechanical coupling factors in the FRMS can be illustrated by the dragging equation as shown in Eq. (1):

$$T - T_L = \frac{J}{9.55} \frac{dn}{dt} \quad (1)$$

where J is the moment of inertia, n is the motor output speed, T denotes the electromagnetic torque, T_L denotes the load torque. When the electromagnetic torque is larger than the load torque, the motor can drive the load. And with the increase of the load torque, the angle between rotor pole and stator rotating magnetic field increase, and the electromagnetic torque subsequently increase until equal to the load torque. Therefore, the stator current increases with the load increasing, and the armature reaction may cause the rise of the air gap flux as well as the stator counter electromotive force.

In this section, the electromechanical coupling dynamic equations of the FRMS, which considers driving motor, transmission system and flexible manipulator as a integrated object, will be constructed based on the electromechanical dynamics analysis approach. During the modeling, assumptions are made as: the iron core saturation, eddy current loss and hysteresis loss are ignored; the air gap is evenly distributed and the

self-inductance as well as mutual-inductance of each phase winding is constant; the rotor does not have damping windings and nor the permanent magnet have damping effect while the form of counter electromotive force is sine curve; the flexible manipulator satisfies the Euler-Bernoulli beam theory and the shear and axial deformation are neglected.

The kinetic energy of the FRMS can be written as

$$E_k = \frac{1}{2}J_R\varphi^2 + \frac{1}{2}J_b\varphi^2 + \frac{1}{2}m_s v_t^2 + \frac{1}{2}\int_0^L \rho A \left(v_t + \frac{\partial w}{\partial t} \right)^2 dx + \frac{1}{2}m_e \left(v_t + \frac{\partial w}{\partial t} \Big|_{x=L} \right)^2 \quad (2)$$

where φ indicates the angular velocity of the motor, J_R is the rotational inertia of the motor shaft and J_b is the rotational inertia of the lead screw which satisfies

$$J_b = \frac{\pi\rho_b D^4 L_b}{32} \quad (3)$$

here L_b , ρ_b and D are the length, density and nominal diameter of the lead screw, respectively.

Based on the movement transitive relation, the relationship between the speed of the base v_t and the angular velocity of the motor φ can be expressed as

$$v_t = \frac{D}{2}\varphi \quad (4)$$

Substituting Eq. (4) into Eq. (2), Eq. (2) can be simplified as

$$E_k = \frac{1}{2}J_R\varphi^2 + \frac{1}{2}J_b\varphi^2 + \frac{1}{8}m_s D^2 \varphi^2 + \frac{1}{2}\int_0^L \rho A \left(\frac{D}{2}\varphi + \frac{\partial w}{\partial t} \right)^2 dx + \frac{1}{2}m_e \left[\frac{D}{2}\varphi + \frac{\partial w}{\partial t} \Big|_{x=L} \right]^2 \quad (5)$$

The elastic potential energy of the FRMS can be written as

$$E_p = \frac{1}{2}\int_0^L EI \left(\frac{\partial^2 w}{\partial x^2} \right)^2 dx \quad (6)$$

Due to the electromechanical coupling effect between the motor and the flexible manipulator, the magnetic field energy should be taken into consideration. The magnetic field energy, produced by the stator current itself, the rotor permanent magnet and the interaction of the stator current and the flux linkage of the rotor, can be expressed as

$$W_m = W_{m1} + W_{m2} + W_{m21} \quad (7)$$

The magnetic energy caused by the stator current can be represented as:

$$W_{m1} = \frac{1}{2}L_u i_u^2 + \frac{1}{2}L_v i_v^2 + \frac{1}{2}L_w i_w^2 + M i_u i_v + M i_v i_w + M i_u i_w \quad (8)$$

where L_u , L_v , L_w express the self-inductance of the three-phase windings, M is the mutual-inductance and i_u , i_v , i_w are the current of the three-phase stator.

Owing to the slot number of each phase is large for the 60° phase distributed windings, the magnetic field energy, caused by the rotor permanent magnet, can be seen as a constant ($W_{m2} = C$).

The magnetic field energy, produced by the interaction of the stator current and the flux linkage of the rotor, can be shown as

$$W_{m21} = i_u \psi_f \cos \theta + i_v \psi_f \cos(\theta - \frac{2}{3}\pi) + i_w \psi_f \cos(\theta + \frac{2}{3}\pi) \quad (9)$$

where θ and ψ_f are the position and flux linkage of the permanent magnet rotor, respectively.

From Eqs. (5)–(7), the Lagrange function of the flexible robot system can be obtained as

$$\begin{aligned} U &= E_k - E_p + W_m \\ &= \frac{1}{2}J_R \varphi^2 + \frac{1}{2}J_b \varphi^2 + \frac{1}{8}m_s D^2 \varphi^2 \\ &\quad + \frac{1}{2} \int_0^L \rho A \left(\frac{D}{2} \varphi + \frac{\partial w}{\partial t} \right)^2 dx + \frac{1}{2} m_e \left[\frac{D}{2} \varphi + \frac{\partial w}{\partial t} \Big|_{x=L} \right]^2 - \frac{1}{2} \int_0^L EI \left(\frac{\partial^2 w}{\partial x^2} \right)^2 dx \\ &\quad + \frac{1}{2}L_u i_u^2 + \frac{1}{2}L_v i_v^2 + \frac{1}{2}L_w i_w^2 + M i_u i_v + M i_v i_w + M i_u i_w + C \\ &\quad + i_u \psi_f \cos \theta + i_v \psi_f \cos(\theta - \frac{2}{3}\pi) + i_w \psi_f \cos(\theta + \frac{2}{3}\pi) \end{aligned} \quad (10)$$

Combining Eq. (10), the Lagrange equation of FRMS can be expressed as [14]

$$\frac{d}{dt} \left(\frac{\partial U}{\partial \dot{r}_k} \right) - \frac{\partial U}{\partial r_k} + \frac{\partial F_h}{\partial \dot{r}_k} = Q_k \quad (11)$$

here F_h is the dissipation functions and Q_k is the non-conservative generalized force.

For the FRMS, the dissipation functions include the dissipation of the mechanical system and electromagnetic system, which can be shown as

$$F_e = \frac{1}{2}R_u i_u^2 + \frac{1}{2}R_v i_v^2 + \frac{1}{2}R_w i_w^2 \quad (12)$$

$$F_m = \frac{1}{2}(B_1 + B_e) \varphi^2 \quad (13)$$

where R_u , R_v , R_w are the resistance of the motor three-phase windings, B_1 is the equivalent viscous damping coefficient of the driving system and B_e is the viscous damping coefficient of the motor. Then, the dissipation functions can be represented as

$$F_h = F_e + F_m = \frac{1}{2}R_u i_u^2 + \frac{1}{2}R_v i_v^2 + \frac{1}{2}R_w i_w^2 + \frac{1}{2}(B_1 + B_e)\dot{\varphi}^2 \quad (14)$$

The non-conservative force is mainly considered as the frictional resistance between the base and the guide rail and can be expressed as

$$Q_i = -\mu m_s g \quad (15)$$

where μ is the friction coefficient between the base and the guide rail and $g = 9.8 \text{ m/s}^2$.

Considering the FRMS is a electromechanical coupling system which contains the electromagnetic system and mechanical system, the Lagrange equation is converted into the Lagrange-Maxwell equations whose form is

$$\begin{cases} \frac{d}{dt} \left(\frac{\partial U}{\partial \dot{e}_i} \right) - \frac{\partial U}{\partial e_i} + \frac{\partial F_h}{\partial \dot{e}_i} = u_i \\ \frac{d}{dt} \left(\frac{\partial U}{\partial \dot{\lambda}_j} \right) - \frac{\partial U}{\partial \lambda_j} + \frac{\partial F_h}{\partial \dot{\lambda}_j} = Q_j \end{cases} \quad (16)$$

Through Eq. (16), the voltage equation of u , v and w stators winding can be respectively obtained as

$$u_1 = L_u \frac{di_u}{dt} + M \frac{di_v}{dt} + M \frac{di_w}{dt} - \varphi \psi_f \sin \theta + R_u i_u \quad (17)$$

$$u_2 = L_v \frac{di_v}{dt} + M \frac{di_u}{dt} + M \frac{di_w}{dt} - \varphi \psi_f \sin(\theta - \frac{2\pi}{3}) + R_v i_v \quad (18)$$

$$u_3 = L_w \frac{di_w}{dt} + M \frac{di_v}{dt} + M \frac{di_u}{dt} - \varphi \psi_f \sin(\theta + \frac{2\pi}{3}) + R_w i_w \quad (19)$$

Defining angular displacement of the motor as the generalized coordinate, According to Eq. (10), it can be obtained that

$$\begin{aligned} & (J_R + J_b + \frac{1}{4}D^2 m_s + \frac{1}{4}D^2 \rho A L + \frac{1}{4}D^2 m_e) \ddot{\varphi} + \frac{D}{2} \int_0^L \rho A \frac{\partial^2 w}{\partial t^2} dx + \frac{D}{2} m_e \frac{\partial^2 w}{\partial t^2} \Big|_{x=L} \\ & = -i_u \psi_f \sin \theta - i_v \psi_f \sin(\theta - \frac{2}{3}\pi) - i_w \psi_f \sin(\theta + \frac{2}{3}\pi) - (B_1 + B_e)\dot{\varphi} - \mu m_s g \end{aligned} \quad (20)$$

Equation (20) reveals the coupling relationship between the angular velocity of the motor and the electromagnetic and mechanical structure parameters of the FRMS.

Based on this, the speed response characteristics of the FRMS under electromechanical coupling effects can be revealed and used to reflect the electromechanical coupling mechanism in the FRMS.

3 Speed Response Characteristics of the FRMS Under Electromechanical Coupling Effects

In order to analyze the electromechanical coupling characteristics of the PMSM speed, a simulation model, which is constructed in Matlab/Simulink, is used to solve Eq. (20) and the speed response characteristics of the FRMS. The structure of the electromechanical coupling simulation model is illustrated in Fig. 2. The main parameters of the FRMS in the electromechanical coupling dynamic simulation are shown in Table 1. The rotational inertia of the lead screw is $J_b = 1.643 \times 10^{-5} \text{ kg}\cdot\text{m}^2$, which are much smaller than that of the shaft. For this, in the simulation analysis, the rotational inertia of the shaft is mainly considered.

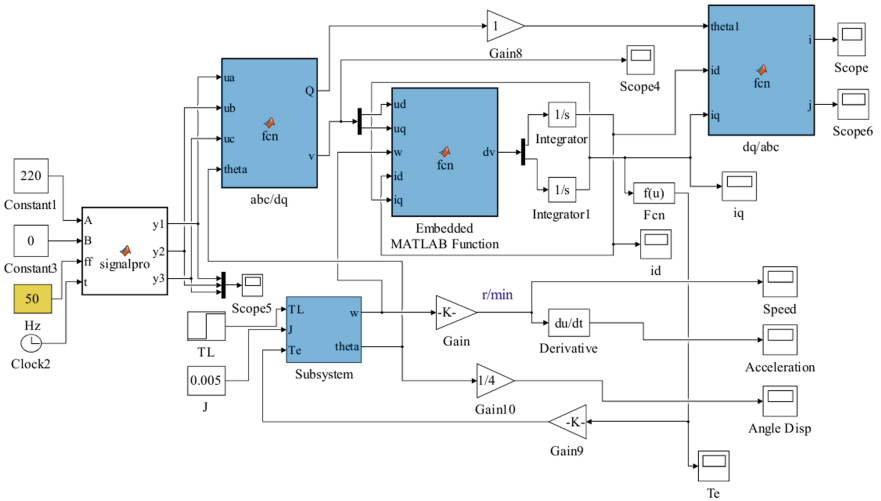


Fig. 2. Simulink model for speeds response of the FRMS under electromechanical coupling effects

The frequencies of the input voltages are defined as $f = 20 \text{ Hz}$, 30 Hz , 40 Hz and 50 Hz . According to the relationship $\phi = 60f/p$, the steady state rotational speed of the PMSM can be got as 300r/min , 450r/min , 600r/min and 750r/min . However, as shown in Fig. 3, under the effect of electromechanical coupling, the speeds are not constant and exhibits certainly fluctuation in the startup process. Moreover, it can be

Table 1. Parameters of the system in the electromechanical coupling dynamic simulation

L	b	h	E	ρ	J_R
400 mm	45 mm	3 mm	25.24 GPa	2030 kg/m ³	0.005 kg·m ²
p	L _b	D	ρ_b	B_e	m _s
4	800 mm	10 mm	7850 kg/m ³	0.0005 kg·m ² /s	1 kg

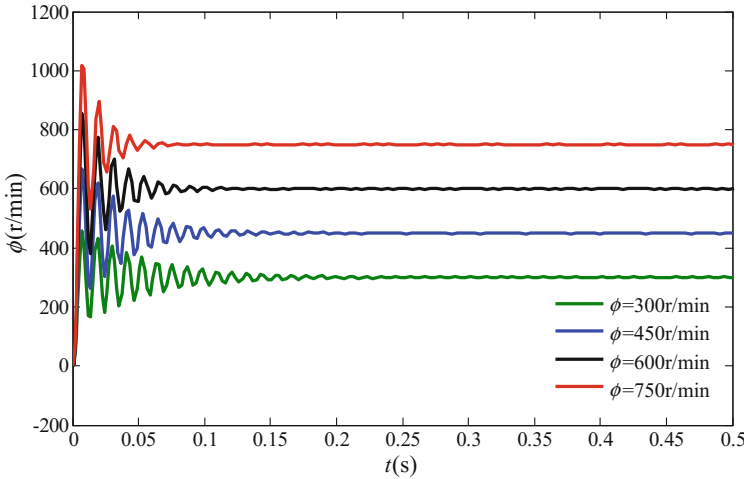


Fig. 3. The speed responses of the FRMS under the electromechanical coupling effects

obtained that the speeds are relatively stable and gradually approach the steady state when the time is more than 0.2 s. Besides, the fluctuation amplitude enhanced with the target speeds.

Figure 4 shows the fluctuation comparison of different target speeds. It can be seen that the fluctuation amplitudes of different rotational speeds exist certain differences but the fluctuation frequencies are similar. In order to uniformly compare the fluctuation level of different rotational speeds, the relatively speed fluctuation is defined as the ratio of the speed fluctuation peak and the target speed, which is expressed as

$$M_p = \frac{\phi_{\max} - \phi_{\infty}}{\phi_{\infty}} \times 100\% \tag{21}$$

Through Eq. (21), the relatively speed fluctuations of 300r/min, 450r/min, 600r/min and 750r/min are calculated as 52.5%, 50.3556%, 42.85% and 35.8667%, which is shown in Table 2. It can be obtained that the relatively speed fluctuations are more obvious for the lower speeds.

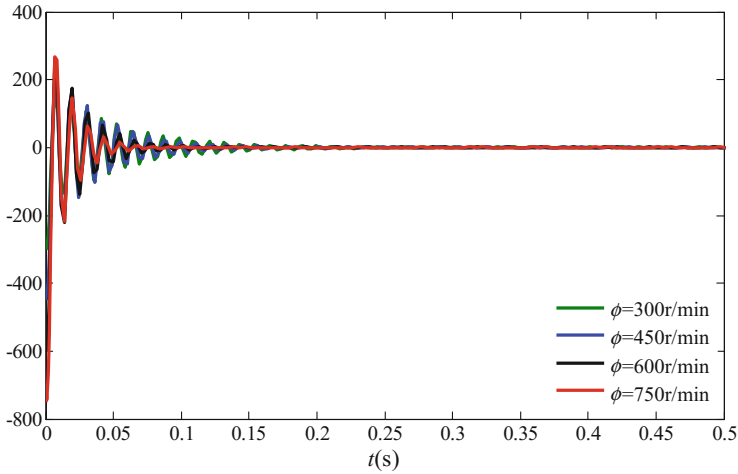


Fig. 4. The speed fluctuations of the FRMS under the electromechanical coupling effects

Table 2. Relatively speed fluctuations of different target speeds

ϕ (r/min)	300	450	600	750
M_p (%)	52.5	50.3556	42.8500	35.8667

4 Conclusions

Regarding the driving motor, transmission system and flexible manipulator as an integrated object, the electromechanical coupling dynamic model was established using the electromechanical dynamics analysis approach. Using the Matlab/Simulink, the dynamic simulation model is constructed to analyze the speed responses of the FRMS under electromechanical coupling effects. The results show that the electromechanical coupling effect have significant influence on the dynamic characteristic of the FRMS, the response speeds are not constant and exhibits certainly fluctuation in the startup process. Moreover, the fluctuation amplitude enhanced with the target speeds while the relatively speed fluctuations are more obvious for the lower speeds. The results are significant for the dynamic and control of flexible robotic manipulators.

Acknowledgements. This research work is supported by the Natural Science Research Project of Higher Education of Anhui Province (no. KJ2017A118), the Project funded by China Post-doctoral Science Foundation (no. 2017M612060) and the Research Starting Fund Project for Introduced Talents of Anhui Polytechnic University (no. 2016YQQ012). The authors sincerely thank the reviewers for their significant and constructive comments and suggestions.

References

1. Dwivedy, S.K., Eberhard, P.: Dynamic analysis of flexible manipulators, a literature review. *Mech. Mach. Theory* **41**, 749–777 (2006)

2. Liu, Y., Li, W., Wang, Y., Yang, X., En, L.: Coupling vibration characteristics of a translating flexible robot manipulator with harmonic driving motions. *J. VibroEng.* **17**(7), 3415–3427 (2015)
3. Kerem, G., Bradley, J.B., Edward, J.P.: Vibration control of a single-link flexible manipulator using an array of fiber optic curvature sensors and PZT actuators. *Mechatronics* **19**, 167–177 (2009)
4. Sen, Q., Bin, Z., Huafeng, D.: Dynamics and trajectory tracking control of cooperative multiple mobile cranes. *Nonlinear Dyn.* **83**(1–2), 89–108 (2016)
5. Bin, Z., Bin, Z.: A modified hybrid uncertain analysis method for dynamic response field of the LSOAAC with random and interval parameters. *J. Sound Vib.* **374**, 111–137 (2016)
6. Liu, Y., Li, W., Wang, Y., Yang, X., Ju, J.: Dynamic model and vibration power flow of a rigid-flexible coupling and harmonic-disturbance exciting system for flexible robotic manipulator with elastic joints. *Shock Vib.* Article ID 541057, 1–10 (2015)
7. Maria, A.N., Jorge, A.C., Ambrósio, L.M., Roseiro, A.A., Vasques, C.M.A.: Active vibration control of spatial flexible multibody systems. *Multibody Syst. Dyn.* **30**, 13–35 (2013)
8. Bin, Z., Jun, L., Sen, Q.: Localization, obstacle avoidance planning and control of cooperative cable parallel robots for multiple mobile cranes. *Robot. Comput.-Integr. Manuf.* **34**, 105–123 (2015)
9. Zhao, J.L., Yan, S.Z., Wu, J.N.: Analysis of parameter sensitivity of space manipulator with harmonic drive based on the revised response surface method. *Acta Astronaut.* **98**, 86–96 (2014)
10. Liu, Y., Li, W., Yang, X., Wang, Y., Fan, M., Ye, G.: Coupled dynamic model and vibration responses characteristic of a motor-driven flexible manipulator system. *Mech. Sci.* **6**(2), 235–244 (2015)
11. Mohsen, D., Nader, J., Zeyu, L., Darren, M.D.: An observerbased piezoelectric control of flexible Cartesian robot arms: theory and experiment. *Control Eng. Pract.* **12**, 1041–1053 (2004)
12. Qiu, Z.C.: Adaptive nonlinear vibration control of a Cartesian flexible manipulator driven by a ball screw mechanism. *Mech. Syst. Sig. Proc.* **30**, 248–266 (2012)
13. Wei, K.X., Meng, G., Zhou, S., Liu, J.W.: Vibration control of variable speed/acceleration rotating beams using smart materials. *J. Sound Vib.* **298**, 1150–1158 (2006)
14. Singiresu, S.R.: *Mechanical Vibration*, 4th edn. Pearson Education Inc., New York (2004)